ARCOS: A DISTRIBUTED AGRICULTURAL REMOTE-SENSING CAMERA SYSTEM ON BOARD A CUBESAT FORMATION

Alexander Bühler*†, Isabel Pitz*†, Max Manthey*, Mert Acikel*, Sebastian Grau*, Enrico Stoll*
* Technische Universität Berlin, Chair of Space Technology, Marchstraße 12-14, 10587 Berlin, Germany; sebastian.grau@tu-berlin.de
† These authors contributed equally to this work.

Abstract

During the 2022/23 winter term, students at the Chair of Space Technology at Technische Universität Berlin developed a multispectral, multi-CubeSat imager formation. The formation was named MIMIR (Multispectral Imager satellite forMation for Inter satellite link and optical downlink demonstRation). A primary mission driver was to address ecological and environmental concerns. The formation consists of eight 1.5U CubeSats - six for imaging and two for payload data transmission. Each of the imaging satellites carries four camera systems with narrow-band spectral filters. This results in 12 redundant spectral channels forming the distributed payload system ARCOS (Agricultural Remote-sensing Cameras On-board Satellites). The chosen channels are located in the visible and near-infrared spectrum. This is motivated by the "red edge" at the boundary between these two spectral ranges. The red edge is a region of rapid change in the reflectance of vegetation - chlorophyll absorbs light in the visible part of the spectrum, but becomes transparent at wavelengths larger than 700 nm. Changes in internal processes and leaf structure affect the absorption of radiation and thus reveal physiological stress in plants. Applying state-of-the-art vegetation health indices, e.g. the NDVI (Normalized Difference Vegetation Index), on the channel data enables monitoring crop health. In collaboration with interested parties in the geo-information technology environment, this extends to the detection of drought and crop disease. To allow for fast stakeholder access to data, an optical downlink is used for data transmission at a high transfer rate. The satellite formation is a distributed system that enables redundant coverage of different spectral bandwidths for stakeholders who put up demands within similar time slots. Picosatellite fluid-dynamic actuators allow more agile changes in attitude for small angles than conventionally used reaction wheels. This enables artificial camera swath width increase aboard the six imaging satellites and lossless data transmission for the inter-satellite data transmission link. At the present time, a system study is being performed, with the objective to achieve a proof of concept by 2024. In this work, the mission design and development state of the MIMIR formation is described, detailing the mechanical, electrical, and attitude determination and control systems.

Keywords

agricultural; CubeSat; remote sensing; multispectral; formation flight

1. INTRODUCTION

In recent years, the relentless pace of climate change and its impact on the global ecosystem have presented pressing challenges. The need for real-time information to address agricultural requirements has surged exponentially, driven by the vast expanses of agricultural land and the evolving dynamics of the natural environment. To keep up with this growing demand, scalability emerges as a logical approach.
To ensure cost-effective scalability within the satellite system, the need for low spacecraft development costs becomes paramount to accommodate a larger number of satellites. In this context, CubeSats assume a crucial role. The CubeSat standard, widely recognized and established in the industry, facilitate a streamlined development process and substantial reductions in launch expenditures. Adherence to these standardised protocols minimizes development timelines and permits the utilisation of readily available CubeSat containers, thereby increasing cost-efficiency and scalability.
The MIMIR project (Multispectral Imager satellite forMation for Inter satellite link and optical downlink demonstRation) - the mission logo is shown in Fig 1 - synthesises these considerations into a multispectral, multi-CubeSat imager formation consisting of eight 1.5U CubeSats. The satellite formation is a distributed system that enables redundant coverage of different spectral bandwidths for stakeholders who put up demands within similar time slots. To guarantee that the considerable data obtained through the imaging payloads can be received at the ground station and, ultimately, the stakeholders, MIMIR employs a laser communication terminal on the two remaining spacecraft for optical

doi: 10.25967/610450

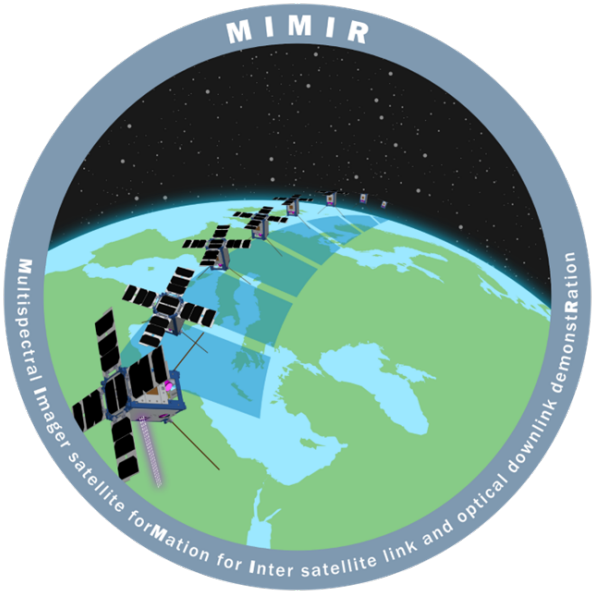

FIG 1. MIMIR mission patch (designer: Johanna Erna Charlotte Teuchert)

payload data transmission at a high transfer rate. The Chair of Space Technology at Technische Universität Berlin has significant heritage of CubeSat technology, including the development of numerous successful missions and components. To utilise these valuable resources, the spacecrafts are based on CubeSat technology readily available at the Chair, and operations are conducted from the in-house ground stations.

This paper presents the mission design and development state of the MIMIR formation, detailing the mechanical, electrical, and attitude determination and control systems.

1.1. Formation design

The initial number of spacecraft in the formation comprises eight 1.5U CubeSats chosen to occupy a 12U deployer. Six of the spacecraft are used for imaging, while two relay satellites are used for optical downlink of payload data. Each of the imaging satellites carries four cameras with a narrow-band spectral filter.

The main design driver for the formation design is the design-to-cost constraint. A complex ejection scheme would induce high costs on the overall launch and early orbit phase with respect to the overall mission cost. Other non-system specific design drivers are the mission lifetime of one year and space debris mitigation guidelines by DLR-RF-PS-001 "Space Debris Mitigation" standards. Further, the following system-specific aspects limit the design of the formation:

- Permanent visual contact between the satellites must be given;
- The line of sight to the imaging target must not be obstructed during imaging;
- The system must use differential drag to reach and hold the final formation;
- Single point of failure resilience for the loss of three-axis attitude control of a single satellite.

The use of differential drag was a requirement stated at the outset of the 2022/23 winter term satellite design project. Whereas the system-specific aspects allow for formation designs of varying complexity, the design-to-cost and mission lifetime constraints imply a simple formation design. Therefore, a single orbital plane formation is chosen. The assumed orbit is Sun-synchronous with an altitude of 540 km. The selected formation places the satellites in a string of pearls, with a constant true anomaly offset between the satellites and the two relay satellites located at the outermost positions. This offset is driven by the single point of failure constraint. It is based on the assumption of a reaction time of one week, after a failure event, to recover a satellite's ability to perform differential drag maneuvers, three-axis attitude control, and precise orbit determination via GPS.

1.2. Differential drag worst-case simulation

To obtain an estimation of the fixed angular distance providing said reaction time of at least one week, a differential drag simulation with a worst-case scenario between two satellites was performed. The result of the simulation, using the explicit Runge-Kutta method of order 5(4) from the SciPy library, is visualised in Fig 2. Differential drag itself makes use of the

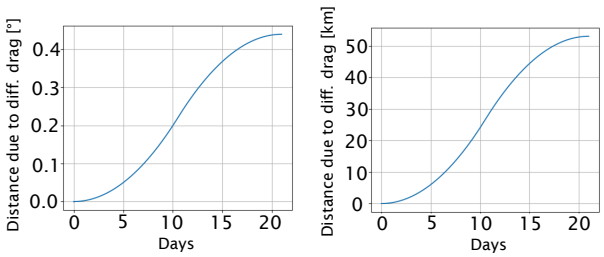

FIG 2. Differential drag worst-case simulation result for a differential drag manouver between two satellites in circular orbits at 540km. Profile swap after 1/2 of 21 days elapsed. Distance of 53.04 km.

different area profiles of the satellites. Due to the 1.5U form factor and the deployable solar arrays, there is a relatively high differential between the two modes. The low-drag profile is achieved by pointing one of the satellite end faces in flight directionand therefore equals approximately 17025 mm². For the high-drag profile, the deployed solar panels are assumed to point in flight direction, which results in an area of approximately 52640 mm². In this simulation, Satellite A is assumed to be stuck in low-drag and Satellite B is assumed to be stuck in high-drag mode. After 11 days, the modes are switched to decrease the relative velocity of the satellites to each other. This resulted in roughly 50 km distance or 0.44°

angular distance between the satellites to ensure this reaction time. Simplifications made were:

- Constant atmospheric density model;
- No solar activity taken into account;
- Permanent differential drag available, undisturbed by downlinks or similar activities.

1.3. Formation phasing simulation

Formation phasing is performed with differential drag only. The result of the formation phasing simulation, again using the explicit Runge-Kutta method of order 5(4) from the SciPy library, is shown in Fig 3. As seen

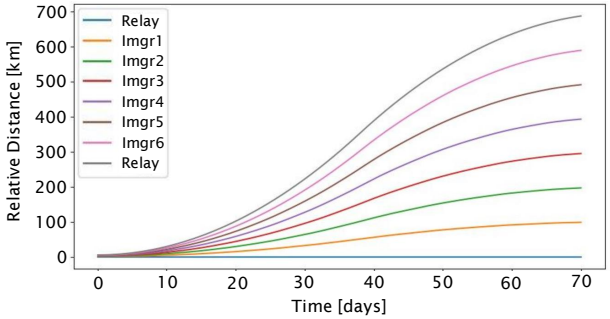

FIG 3. Formation phasing simulation result

in Fig 3, the simple phasing algorithm to determine the drag profile solely based on the neighbouring satellites was implemented into the simulation. The simulation aims to establish the 50 km separation target between the satellites, which incorporates two final criteria:

- The distance between each pair of neighbouring satellites must be within 50km +/-1 km;
- The rate of change must be below an arbitrary threshold indicating the first derivative of the position.

Since the utilised algorithm is basically a proportional control, it does not take into account first or second order derivatives of the position. Therefore, a large, unevenly distributed overshoot is visible. This overshoot is estimated to be corrected over time. It nevertheless is not desirable. As the behaviour is linearly scalable due to the simplistic models used for simulation, it is possible to deduct an estimation of the lowest boundary of the phasing time. It would take at least 40 days to phase the satellites in position under perfect conditions while keeping safety margins for the distance as a priority. There are existing algorithms which are applicable for phasing as well as station keeping, such as the algorithm proposed by Foster et. al in [1]. This algorithm enables slot assignments in a fixed angular frame on a single orbit and takes first and second order derivatives into account to avoid overshooting.

2. PAYLOAD SYSTEM

Six of the spacecrafts are used for imaging. Each carry four camera systems with a narrow-band spectral filter, which can be used for remote sensing to handle tasks that address ecological and environmental concerns. The satellite formation is a distributed system that enables redundant coverage of different spectral bandwidths for stakeholders who put up demands within similar time slots. The chosen channels are located in the visible and near-infrared spectrum. This is motivated by the "red edge" at the boundary between these two spectral ranges. The red edge is a region of rapid change in the reflectance of vegetation - chlorophyll absorbs light in the visible part of the spectrum, but becomes transparent at wavelengths >700 nm. Changes in internal processes and leaf structure affect the absorption of radiation and thus reveal physiological stress in plants. Applying state-of-the-art vegetation health indices, e.g. the NDVI (Normalised Difference Vegetation Index), on the channel data enables monitoring crop health [2]. In collaboration with interested parties in the geo-information technology environment this extends to the detection of drought and crop disease, for instance. To provide redundancy, each spectral channel is included twice within the formation, on two independent satellites. This results in a total of 12 spectral channels distributed across the imaging satellites. The imaging system including optics design and payload data handling is closely adapted from the system developed for the NanoFF mission of Technische Universität Berlin. Due to launch in 2024, the NanoFF mission consists of two CubeSats carrying four camera systems each.

3. ATTITUDE DETERMINATION AND CONTROL SYSTEM

The attitude determination and control system (ADCS) was designed around the design driver of the optical downlink, which allows for fast stakeholder access to data. The scenario of a nanosatellite establishing an optical downlink was assessed with respect to its feasibility, as part of the ADCS design, by Bühler in [3]. An emphasis was put on hardware readily available and developed at Technische Universität Berlin, namely picosatellite fluid-dynamic actuators (pFDAs), developed by Grau in [4], and star sensors, developed by Korn in [5].

3.1. Attitude determination and control requirements derivation

The ADCS requirements were derived from a review of the state of the art and from an orbit and attitude analysis.

3.1.1. Review of the state of the art

A review of the research and technology context with regards to similar missions identified and compared two different approaches for realising optical communication aboard nanosatellites. One approach was present within the PIXL-1 mission, led by Deutsches Zentrum für Luft- und Raumfahrt

(DLR) [6]. This mission had sought to demonstrate the CubeLCT laser communication terminal aboard a 3U CubeSat, which was launched in January 2021 [6] [7]. A second approach was present within the Optical Communication and Sensor Demonstration (OCSD) mission, launched in 2017 [8] and consisting of two 1.5U CubeSats [9]. As part of an explicit low-complexity approach, the CubeSat slewed by itself to point the laser transmitter towards the ground station. The key enabling elements for this were two highly precise star trackers and three reaction wheels [9]. This review resulted in a differentiation of the two approaches with respect to the requirements that they imposed on their respective ADCS. PIXL-1 set an attitude control error of $<1^\circ$ for its ADCS to compensate, while relying on the fine pointing assembly inside its CubeLCT to manage the remaining control inaccuracy [6]. On the other hand, OCSD established comparatively very stringent requirements on both attitude determination and control errors of $<0.015^\circ$ each, expecting these requirements to be met by the sensor and actuator suite [9]. Further, a challenge specific to this scenario that had been explicitly mentioned in [9] were the high angular rates that the nanosatellite is subjected to during flight over an optical ground station, making precise attitude determination with star trackers challenging due to smearing of star tracker images.

3.1.2. Orbit and attitude analysis

Orbit and attitude analysis was performed to define an orbit on which a nanosatellite, equipped with pFDAs, would experience worst-case angular rates while implementing optical communication with a ground station. The focus was put on the estimation of the maximum absolute value of the angular rate for different orbit heights and different optical ground stations. A contour plot for the Haleakala optical ground station, located in Hawaii, is shown in Fig 4. This resulted in a set of orbit models from which

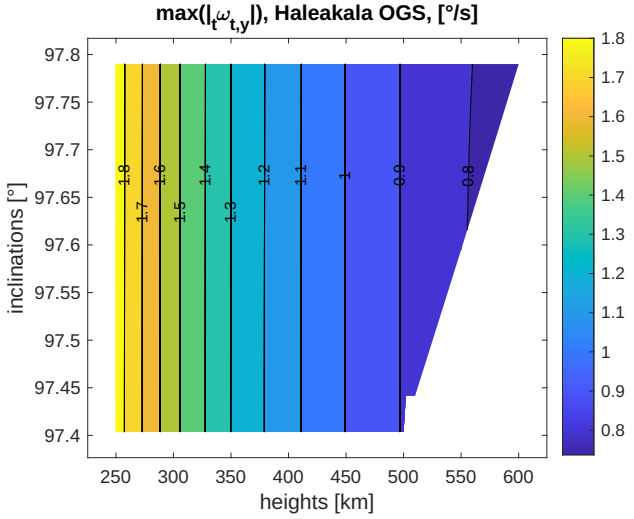

FIG 4. Worst-case angular rates for Haleakala optical ground station [3]

an orbit featuring a realistic worst-case angular rate value was selected. The determined worst-case angular rate, for an orbit altitude of 500 km after a mission lifetime of one year, is $0.89\frac{^\circ}{s}$.

3.1.3. Determined requirements

The requirements on pointing accuracy and pointing knowledge accuracy were derived from the results of the review of current research and technology and of the orbit and attitude analysis in [3]. A defining requirement is that the angular rates about the satellite target reference frame y-axis must not exceed the maximum value of $0.89\frac{^\circ}{s}$ that had been determined in the orbit and attitude analysis. This maximum value is valid only if the ground station is not located closer to the equator than Haleakala ground station and the spacecraft altitude has not decayed to less than 500 km, which were assumptions taken in the orbit and attitude analysis. It was decided to set the attitude control accuracy error threshold to $<0.1^\circ$, one order of magnitude below that of PIXL-1. It was assessed that a control accuracy $<1^\circ$ would be too inaccurate for the optical downlink scenario. At the same time, the attitude determination accuracy error threshold was set to $<0.1^\circ$, one order of magnitude above that of the Optical Communication and Sensor Demonstration (OCSD) mission. The reason for this was that it was estimated, after viewing the requirements on the Technische Universität Berlin (TU Berlin) star tracker developed in [5], stating that the star camera shall deliver attitude determination with an error of 0.1° and deliver star images up to an angular rate threshold value of $2\frac{^\circ}{s}$ that a requirement on attitude determination accuracy below 0.1° was not realistic.

3.2. Controller parameter search

Controller parameters for the pFDAs were then determined in a parameter search within a dynamics simulation. To this end, dynamics simulation scripts that had been written by Grau et al. in [10], taking into account the dynamics of the pFDAs, were used, and extended with a controller parameter search in [3]. Results of the controller parameter search can be seen as contour plot as function of the two PD controller parameters K_d and K_p in Fig 5. Figure of merit 1 was defined as being equal to the maximum value of the error angle, i.e. the attitude accuracy error between the laser communication terminal line of sight and the optical ground station. The use of the pFDAs leads to a limitation of the attitude accuracy error, i.e. the error angle, below a defined threshold of $< 0.1^\circ$, reaching a maximum value of 0.007°, as shown in Fig 6. This in turn leads to the preliminary assessment that, using pFDAs, and under the assumption that the star trackers fulfil their requirements, a mission implementing an optical downlink aboard a nanosatellite with the pFDAs and star trackers developed at TU Berlin is indeed feasible.

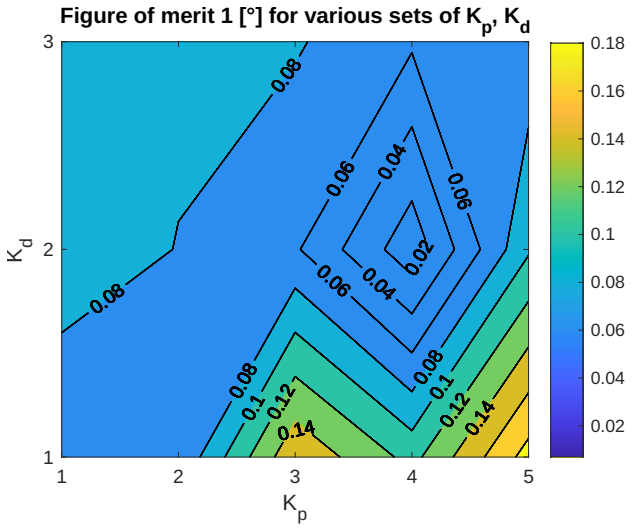

FIG 5. Figure of merit 1 (maximum value of error angle) as a function of controller parameters K_p, K_d (first iteration) [3]

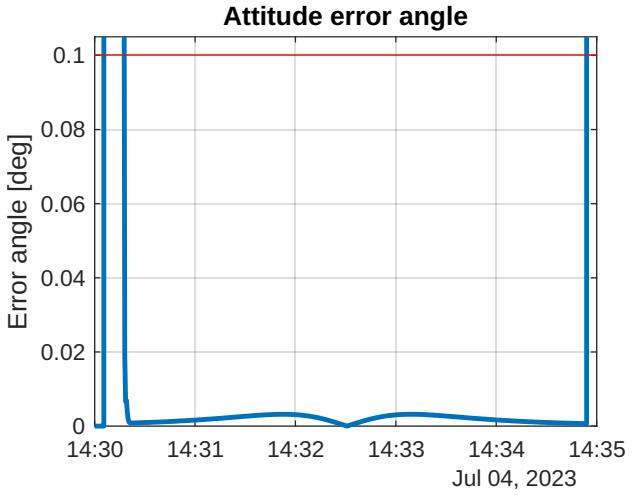

FIG 6. Error angle for selected controller parameters $K_p = 4, K_d = 2$ [3]

4. STRUCTURES AND MECHANISMS SYSTEM

The structures and mechanisms system (SMS) is designed around the design drivers of design-to-cost philosophy, rideshare constraints with launchers, and TU Berlin Chair of Space Technology CubeSat technology heritage.

4.1. Preliminary structural design

Given the academic background of this mission design, the design-to-cost philosophy was a primary constraint that had to be adhered to. Accordingly, the CAD mechanical design is constructed in observance of sheet metal forming processes. Using these methods, cost reduction is expected when compared to the use of e.g. milling processes, both in terms of production costs and in terms of material saving. An image of the CAD design for the relay satellite, with notable components labelled, is shown in Fig 7. Instead of using a single milled piece for the satellite

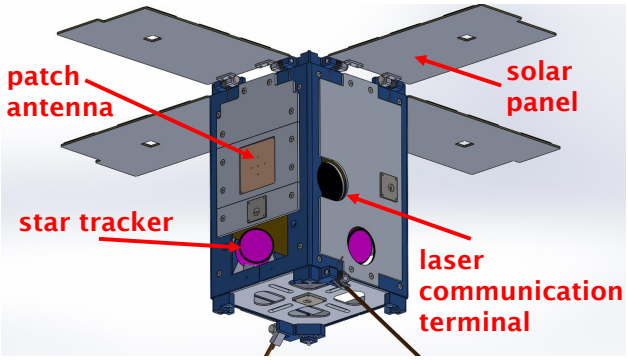

FIG 7. Satellite CAD model

chassis, separate elements were designed. These elements include two lateral struts, and a top and bottom plate. Images of the CAD realisations of these elements are shown in Fig 8 and Fig 9. Since the

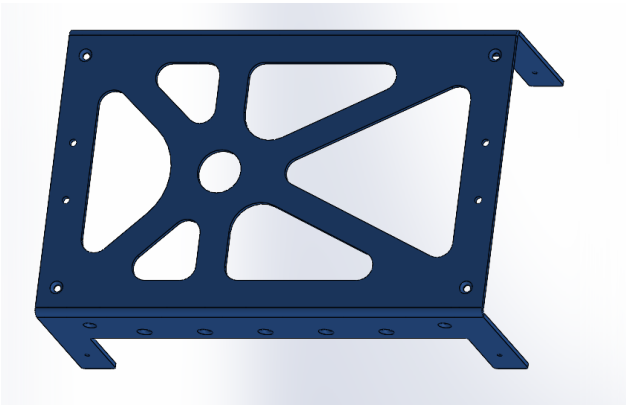

FIG 8. Satellite lateral strut sheet metal CAD model

lateral structure strut only has a thickness of 1.5mm and both the top and bottom plates only have a thickness of 1 mm, beadings are incorporated into the top and bottom plates to increase stiffness and flexural strength. The parts are fastened by M2 Torx screws in threaded holes of both the lateral structure

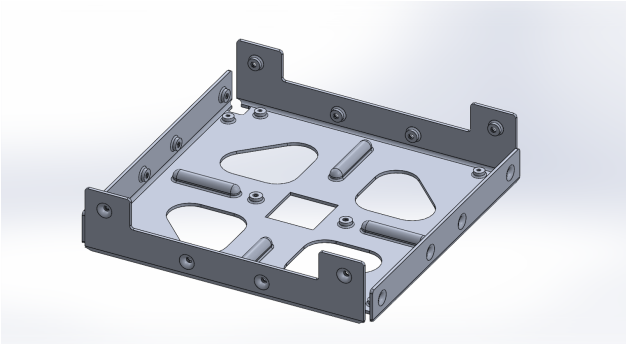

FIG 9. Satellite top plate sheet metal CAD model

struts and the top/bottom plates. The manufacturing of those holes is done via punching and thread forming. This has the advantage that the holes gain length through the punching, thus enabling a surface that then can be formed into a thread. The latter is also advantageous since the material is not cut in this area, but rather pressed and rolled. This does not produce notches which would decrease the material strength, but instead increases the material strength. As the development of MIMIR is built on the technological heritage of TU Berlin, the formation is based on CubeSat technology readily available at TU Berlin. The CubeSat design specification (CDS) was chosen to be adhered to, with the CDS mainly being of use to CubeSat developers as a guideline only. The design has to ultimately meet the requirements set by launch service providers. The CDS provides requirements so that the spacecraft may be compatible with as many CubeSat dispensers and launch opportunities as possible. With this in mind, the 1.5U CubeSat format is selected as it allowed for the integration of eight such satellites, i.e. the entire formation, in a single Exolaunch 12U dispenser [11].

4.2. Preliminary mechanisms design

The mechanisms for the deployment of both the solar arrays and the UHF antennas are designed to efficiently use the limited space on the surface of the 1.5U Cubesats. A similar approach to the TU Berlin Nanosatellites in Formation Flight (NanoFF) design was chosen, which proved to be effective and satisfies the use of heritage from the Chair of Space technology. Following the CDS, at least 75% of the rail should be in contact with the dispenser rails and 25% of the rails may be recessed. This allows the rail standoffs to be designed as separate milled parts that can be fastened via M2 Torx screws to the top and bottom plates. The special feature of the rail standoffs is that they also accommodate the separation mechanisms in form of a spring plunger, the deployment switches, the deployment mechanisms for the solar arrays in form of a spring hinge, and the deployment mechanisms for the UHF antennas. The rail standoffs for the UHF antennas and the solar arrays are shown in Fig 10 and Fig 11, respectively.

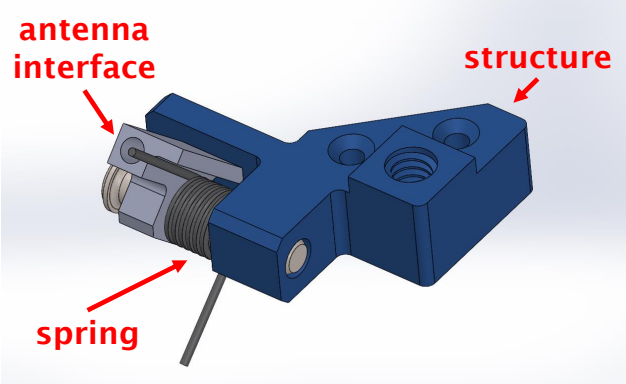

FIG 10. UHF antenna standoff CAD model

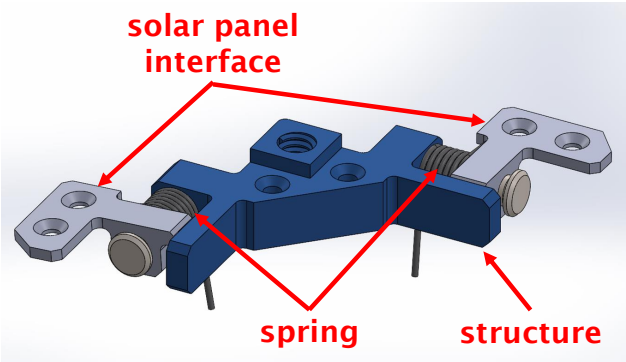

FIG 11. Satellite solar array CAD model

4.3. Interfaces with subsystems

The next step in the design process is to integrate the structure and mechanisms system (SMS) with the other subsystems, such as the Electrical Power System (EPS), Thermal Control System (TCS), Attitude Determination and Control System (ADCS), Onboard Data Handling (OBDH), Communications System (COMMS), and the imaging payload. At the current stage in the development process, a broad allocation of the subsystems in the satellite's inner envelope is determined. In the following, important interfacing aspects that the future project team should take into account in future design iterations are elaborated upon. One important aspect of interfacing is ensuring that the dimensions of the SMS allow for proper integration with the other subsystems. For example, the size and location of mounting holes for the EPS, OBDH, ADCS, COMMS PCBs, and payload must be carefully considered to ensure proper alignment and functionality. Additionally, any connectors or harnesses required for communication between subsystems must be accounted for in the SMS design. In terms of the EPS, the SMS must provide adequate support for the solar panels and their deployment mechanisms. The solar cells are mounted on winged panels attached to the chassis using spring hinges, which are

integrated into the rail standoffs described earlier. The hinges are spring-loaded to ensure proper deployment upon release. The SMS must also provide mounting points for the EPS battery, as well as any additional electronics required for the EPS PCU system. For the TCS, the SMS must provide proper thermal insulation and ensure that there is sufficient space for the TCS components. This will include mounting points for the TCS radiator, as well as any additional insulation required to maintain the desired temperature range within the satellite. For the ADCS, the SMS must provide mounting points for the pFDAs, magnetorquers, sun sensors, and in the case of the relay satellite, star sensors. The mounting points must be designed to ensure proper alignment and stability of the ADCS subsystem. The preliminary emplacement of the star sensors that had been determined within the preliminary orbit and attitude analysis that had been discussed in Sec. 3 will require revision. For the OBDH, the SMS must provide adequate space for the onboard computer and associated electronics. The SMS must also provide mounting points for any sensors or other devices required for OBDH functions. For the COMMS, the SMS must provide mounting points for the S-Band patch antennas and UHF antennas, adequate space for the transceiver module, and in the case of the relay satellite, adequate space for the laser communication terminal used for the optical downlink. For the Guidance, Navigation and Control (GNC) system, the SMS must provide adequate space for the retroreflectors used in satellite laser ranging and ensure proper alignment for accurate measurements. Unfortunately, due to space constraints the tetrahedral configuration of retroreflectors is not possible. Therefore, the SMS must ensure that there is enough space for at least one retroreflector per side. Finally, for the payload, the SMS must provide mounting points and any necessary interface connectors for the camera sensors and electronics, like the PDH. This will ensure proper alignment and connection of the payload subsystem with the rest of the satellite.

5. ELECTRICAL POWER SYSTEM

The primary constraint on the electrical power system (EPS) was the mission lifetime of one year. The EPS was then designed to provide its four main functionalities over this entire mission lifetime. These four functionalities are power generation, storage, conditioning, and distribution. The power consumption was calculated for each mode that the satellites would be placed in. For the relay and the imaging satellite, respectively, the main power consumers were the laser communication terminal and the camera unit, with the laser communication terminal alone consuming 10 W of peak power. The camera unit was expected to consume 4 W of power, as well as the S-Band communication unit. Since the power budget only represents power consumptions without time dependencies, further calculations along with activity time for each imager and relay mode during one orbit were necessary to determine the energy budget and the required battery capacity and required solar cell power generation capability. Another important part of EPS project work consisted of gathering more realistic values for solar cell power generation capability since solar cell degradation, non-optimal angle between solar panel vector, and sun vector and variable temperature environment can negatively affect the solar cell power generation capability during mission lifetime. Two steps were necessary:

- Simulating an orbit during sun time for relay and imager;
- Analysing thermal data for solar cells since realistic temperatures do not match ideal temperatures for the solar cells.

The orbit was simulated within the preliminary orbit analysis that formed the basis for the orbit analysis discussed in Sec. 3. Thermal Desktop [12] thermal simulations showed values for heat generation and temperature in the solar cells during sun exposure, as shown in Fig 12. With the results for both steps

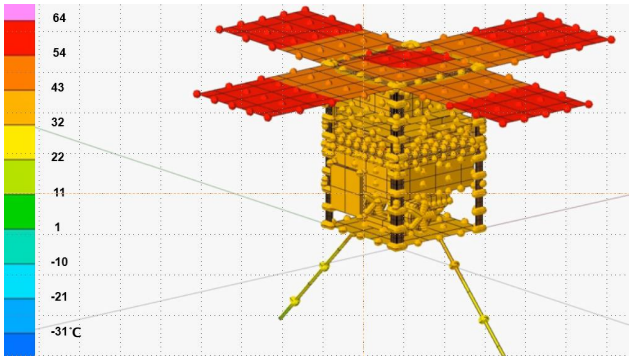

FIG 12. Sun exposure thermal simulation

mentioned above, the realistic solar cell power generation capability could be calculated. The current design for power generation and storage are sufficient to establish the required energy needs of MIMIR. The product architecture for both the relay and imaging satellites were similar to other missions developed at TU Berlin, such as the BEESAT or NanoFF missions.

6. INFORMATION AND DOCUMENTATION MANAGEMENT

As the MIMIR project is a collaborative effort of student projects and theses and is intended for further development in changing team scenarios, clear information and documentation management is crucial. Therefore, the distributed version control system Git along with the Git host service GitLab were used from the beginning of the project. All project-related information is saved in the Git repository. This allows for the technical documentation, along with its development history, to be stored and permanently

accessible to future university teams. To work as a team in a cohesive way, guidelines are set for working with Git. These guidelines are documented in the GitLab Wiki. GitLab Issues and tasks are created for managing project work, with guidelines to ensure a uniform workflow. All issues are given clear milestones, Issues are labelled with the relevant topics and assigned a responsible member. This ensures the Issues are processed. Closing an Issue is only done with a commented reason. The GitLab Wiki provides team information, documentation and a protocol of each project session. Informal information exchange is performed using a chat system hosted by TU Berlin. With these guidelines and work procedures it is ensured that no information gets lost when team constellations change, which will happen regularly due to the university context of this mission.

7. CONCLUSION

During the 2022/2023 winter term and 2023 summer term, students at Technische Universität Berlin developed the CubeSat formation mission MIMIR. At the present time, a system study is being performed, with the objective to achieve a proof of concept by 2024. The presented mission concept addresses the need for real-time information to meet agricultural requirements using a low-cost, scalable formation mission approach.
The 12 spectral channels distributed redundantly over the six imager CubeSats are located in the visible and near-infrared spectrum. Applying state-of-the-art vegetation health indices on data in this spectral range enables monitoring crop health. In collaboration with interested parties in the geo-information technology environment this extends to the detection of drought and crop disease, for instance. To allow for fast stakeholder access to data, an optical downlink is used for data transmission at a high transfer rate. The use of an optical requires stringent pointing accuracy. These requirements are met using picosatellite fluid-dynamic actuators and star trackers developed at Technische Universität Berlin. The picosatellite fluid-dynamic actuators allow for more agile changes in attitude for small angles than conventionally used reaction wheels. This combination enables artificial camera swath width increase aboard the six imaging satellites and lossless data transmission for the inter-satellite data transmission link. The CubeSat formation is arranged as a string of pearls, with the two relay satellites at the outermost positions. The structures and mechanisms system (SMS) was designed around the design drivers of design-to-cost philosophy, rideshare constraints with launchers, and TU Berlin Chair of Space Technology CubeSat technology heritage. Accordingly, the mechanical design was constructed in observance of sheet metal forming processes to be employed in a later physical realisation. Using these methods, cost reduction is expected when compared to the use of e.g. milling processes and in terms of material saving. The combination of the chosen sheet metal principle and using CubeSat standards facilitates scalability of the satellite formation for future mission needs. The current design for power generation and storage are sufficient to establish the required energy needs of MIMIR.
To allow for further development aligning with the dynamic nature of university projects involving student, strict information and documentation management systems are followed. To summarise, the MIMIR project is the next logical step towards a real-time, multi-spectral Earth imaging system.

8. ACKNOWLEDGEMENTS

The MIMIR project would not have been possible without the contribution of all its team members:
- Isabel Pitz (project management)
- Eric Rübhagen (systems engineering)
- Mert Acikel (electrical power system)
- Alexander Bühler (attitude determination and control system)
- Mary Nathina Kanisias (guidance, navigation, and control system)
- Alexander Bauer (guidance, navigation, and control system)
- Ersin Alsac (communications system)
- Christopher Barz (onboard data handling)
- Max Manthey (thermal control system)
- Burkan Akyil (structures and mechanisms system)

References

[1] Cyrus Foster, Henry Hallam, and James Mason. Orbit determination and differential-drag control of planet labs cubesat constellations. *arXiv preprint arXiv:1509.03270*, 2015.

[2] A.-K. Mahlein, T. Rumpf, P. Welke, H.-W. Dehne, L. Plümer, U. Steiner, and E.-C. Oerke. Development of spectral indices for detecting and identifying plant diseases. *Remote Sensing of Environment*, 128:21–30, 2013. ISSN: 0034-4257. DOI: https://doi.org/10.1016/j.rse.2012.09.019.

[3] Alexander Bühler. System design of a highly agile, highly precise attitude determination and control system for nanosatellites. Master's thesis, Technische Universität Berlin, 2023.

[4] Sebastian Grau. *Contributions to the Advance of the Integration Density of CubeSats*. PhD thesis, Technische Universität Berlin, 2019.

[5] Nikolas Moritz Korn. *Entwicklung eines hochintegrierten, multifunktionalen Sternkamerasystems für Pico-und Nanosatelliten*. PhD thesis, Technische Universität Berlin, 2022.

[6] Benjamin Rödiger, Christian Menninger, Christian Fuchs, Lukas Grillmayer, Saskia

Arnold, Christoph Rochow, Philipp Wertz, and Christopher Schmidt. High data-rate optical communication payload for CubeSats. In *Laser Communication and Propagation through the Atmosphere and Oceans IX*, volume 11506, pages 12–24. SPIE, 2020.

[7] eoPortal. PIXL-1. (Last accessed on: 01-09-2023). https://www.eoportal.org/satellite-missions/pixl-1.

[8] eoPortal. Aerocube 7-ocsd-a (aerocube 7 - optical communication and sensor demonstration-a). (Last accessed on: 06-08-2023). https://www.eoportal.org/satellite-missions/aerocube-ocsd.

[9] TS Rose, DW Rowen, SD LaLumondiere, NI Werner, R Linares, AC Faler, JM Wicker, CM Coffman, GA Maul, DH Chien, et al. Optical communications downlink from a low-earth orbiting 1.5 U CubeSat. *Optics express*, 27(17):24382–24392, 2019.

[10] Sebastian Grau, Sascha Kapitola, Sascha Weiss, and Daniel Noack. Control of an over-actuated spacecraft using a combination of a fluid actuator and reaction wheels. *Acta Astronautica*, 178:870–880, 2021.

[11] EXOLAUNCH GmbH. Exopod - cubesat deployer - 12u. (Last accessed on: 28-08-2023). https://exolaunch.com/exopod.html#1.

[12] Inc. C&R Technologies. Thermal desktop. (Last accessed on: 28-08-2023). https://www.crtech.com/products/thermal-desktop.